

Supplementary information

Exploring the Impact of Cetyltrimethylammonium Bromide Surfactant on Electrochemical Performance of Tungsten Oxide Thin Films

Munazza Razzaq^a, Muhammad Saifullah^{b*}, Ramzan Akhtar,^b Muhammad Jawad Khan,^a Zahid Imran,^{a**} Muhammad Rehan,^c Ahsan Jamal,^b Sajid Iqbal,^d Mohsin Ali Raza Anjum,^b and Sheeraz Mehboob^b

^aDepartment of Physics, COMSATS, Islamabad, Pakistan

^bChemistry Division, Pakistan Institute of Nuclear Science and Technology (PINSTECH), Islamabad, Pakistan

^cPhotovoltaic Research Department, Korea Institute of Energy Research (KIER), Daejeon, South Korea

^dDepartment of Nuclear and Quantum Engineering, Korea Advanced Institute of Science and Technology, Daejeon, South Korea

Corresponding authors.

*saifullahkier@gmail.com (Muhammad Saifullah).

**zahid.imran@comsats.edu.pk (Zahid Imran).

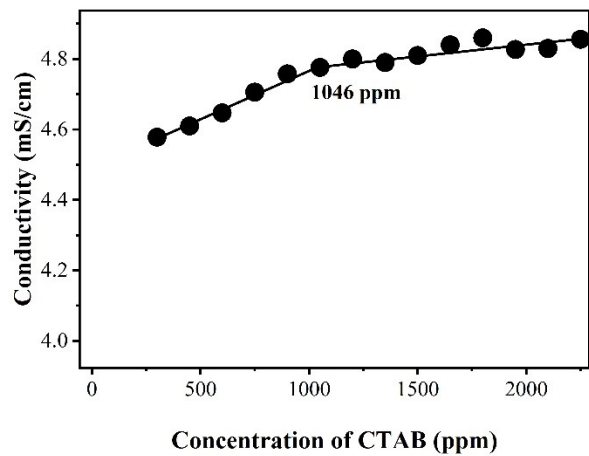


Fig. S1. Conductivity of solution as a function of CTAB concentration. In the reaction medium, first 3 M HCl was added to lower its pH to 2-3 and then CTAB addition was performed in steps to increase the overall concentration of CTAB.

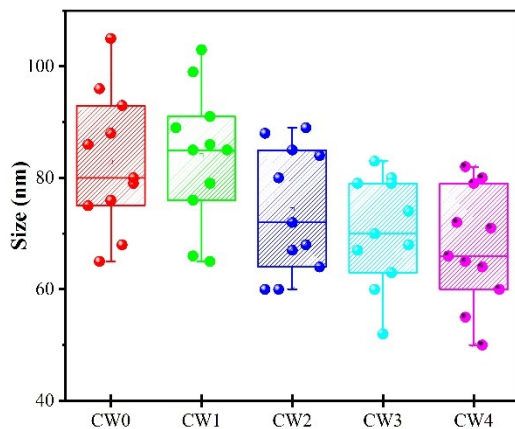


Fig. S2. Box whisker plot showing the particle size distribution determined from SEM surface images of WO_3 thin films prepared with different CTAB/W molar ratios.

BET Analysis of WO_3 NPs:

The specific surface area and average pore size of the pristine WO₃ nanoparticles (NPs) (CW0) and the best WO₃ NPs sample (CW4), as determined using the multipoint Brunauer–Emmett–Teller (BET) analysis, are summarized in Table S1. The N₂ adsorption-desorption isotherms of CW0 and CW4 WO₃ NPs are depicted in **Fig. S3**. According to IUPAC classification, the N₂ adsorption-desorption isotherm of CW0 (**Fig. S3(a)**) conforms to type-III, with a minimal hysteresis between adsorption and desorption curves, indicating its mesoporous nature with a wide distribution of pore size ranging from micro to mesopores.¹ The N₂ adsorption-desorption isotherm of CW4 NPs, shown in **Fig. S3(b)**, has a hysteresis between adsorption and desorption curves typical of type-IV, mainly having mesopores.² The specific surface area of CW4 NPs is 20.02 m²/g, exceeding the surface area of CW0, which is 14.71 m²/g. The higher surface area of CW4 NPs can be attributed to its comparatively better redox activity for Li⁺ ions. The average pore size of CW4 was 3.40 nm, slightly less compared with the 5.39 nm pore diameter of CW0.

Table S1. BET analysis of pristine (CW0) and the best sample (CW4).

Sample ID	Specific S.A (m ² /g)	Total pore volume	Average pore size (Å)
		(cm ³ /g) @ 0.99	@ 0.99
CW0	14.71	0.0397	53.95
CW4	20.02	0.0341	34.03

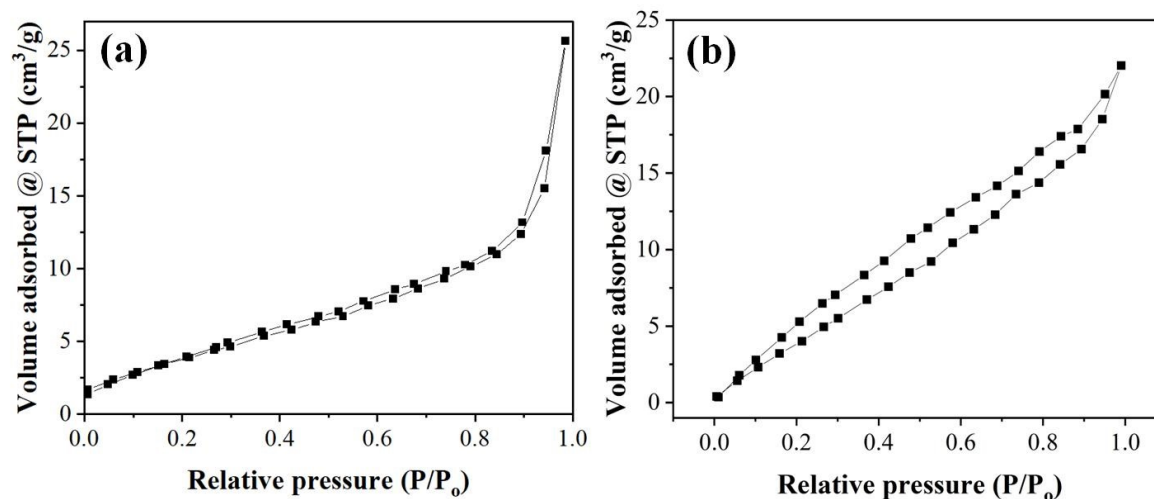


Fig. S3. BET adsorption/desorption curves of CW0 (a) and CW4 (b).

Electrocatalytic performance of WO₃ thin films:

The pristine thin film (labeled as CW0) and the best CTAB-modified thin film (labeled as CW4) were tested for hydrogen and oxygen evolution reactions (HER/OER) in aqueous 1M KOH electrolyte and 0.5 M H₂SO₄ using a three-electrode system. Due to the instability of thin films in acidic media, their performance for electrocatalytic water splitting was subsequently tested in alkaline media. The working electrode was prepared as a thin film against, with the reference Ag/AgCl electrode and graphite rod counter electrode completing the setup. The potential windows for HER and OER, with a sweep rate of 5 mV/s studies, were -0.8 to -1.5 V and 0.15 to 0.85 V, respectively.

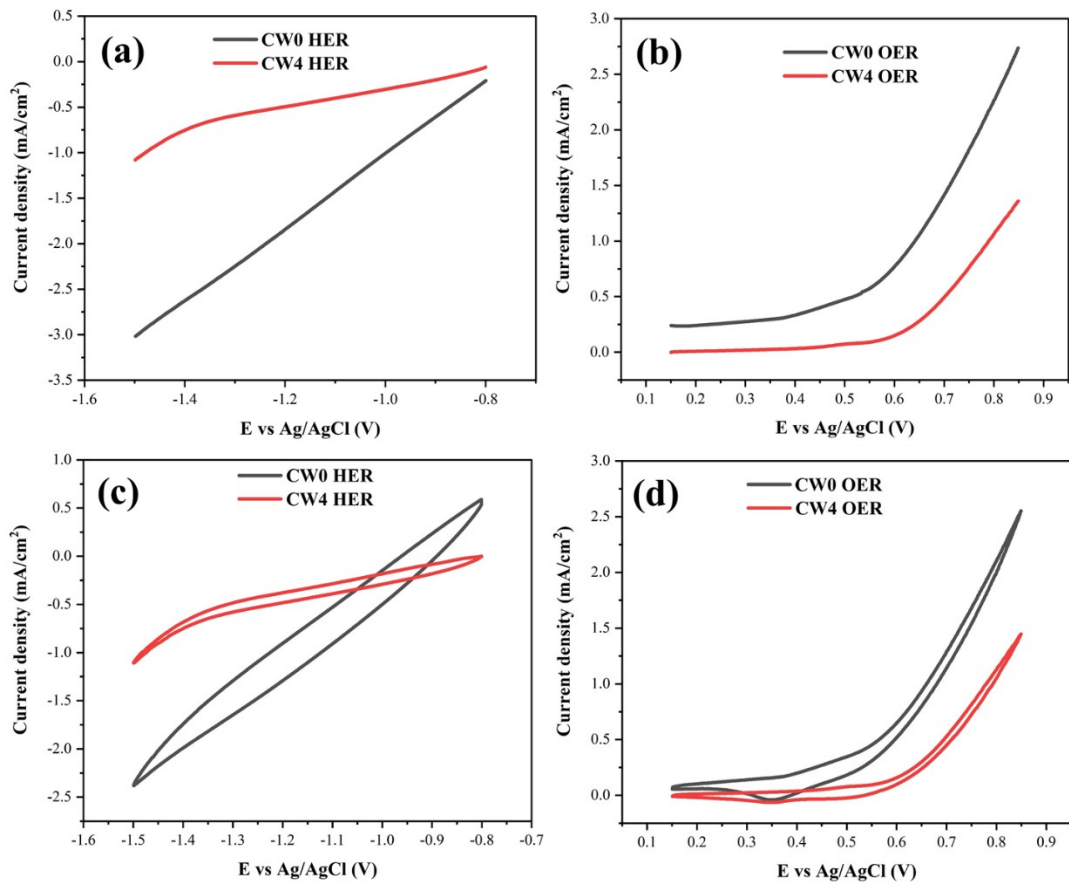


Fig. S4. The LSV (a) & (b) and CV (c) & (d) curves for CW0 and CW4 for OER/HER in aqueous (1M KOH) were recorded at a scan rate of 5 mV/s.

The linear sweep voltammograms (LSV) and cyclic voltammograms (CV) at 5 mV/s of CW0/CW4 samples for OER/HER are depicted in **Fig. S4(a) & (b)** and **Fig. S4(c) & (d)**, respectively. The WO_3 thin films grown on FTO showed poor electrocatalytic performance, particularly for both HER and OER. However, their electrochemical application for water splitting can be further tuned by growing them on other conductive substrates such as metallic (Ni, Cu, etc.) foams, nitrogen-doped carbon materials like graphene, carbon nanotubes, and carbon cloth.

References

1. A. Mukhtar, N. Mellon, S. Saqib, S.-P. Lee and M. A. Bustam, *SN Appl. Sci.*, 2020, **2**, 1232.
2. K. S. Merija, K. M. Rahulan, R. A. Sujatha and N. A. L. Flower, *Front. Energy Res.*, 2023, **11**, 1139604.